Optimization of FIBMOSs Through 2-D Device Simulations

J. Kang, D. K. Schroder and D. P. Pivin Jr.
Dept. of Electrical Engineering/Center for Solid State Electronics Research
Arizona State University, Tempe, AZ, USA, jkang@asu.edu

ABSTRACT

Channel engineering can enhance the performance of MOSFETs. Focused ion beam (FIB) implant technology is one approach for such channel engineering. We have investigated FIB and present a sophisticated optimization technique for FIB MOSFETs (FIBMOS) using 2-D device simulations and 3-D threshold voltage (V_T) contour mapping. In the course of this study, we have discovered that FIBMOSs exhibit higher drain current than normal MOSFETs. We studied both single-step and two-step implanted devices (TSFIBMOS). TSFIBMOS has higher drain current and better performance at low supply voltages. The advantages of FIBMOSs and TSFIBMOSs are presented by benchmarking against normal MOSFETs in the core device performance area.

Keywords: Channel engineering, sub-micron MOSFETs, short channel effect, focused ion beam, hot-carrier degradation.

1 INTRODUCTION

Focused Ion Beam is commonly used during failure analysis and circuit/mask repair.[1, 2] FIB also has the potential for channel engineering due to its ability of implanting very narrow doping regions. The resolution of FIB can be as low as 40 nm allowing dopants to be placed anywhere in the channel. Shen *et al*. employed a FIB to fabricate a FIBMOS with a narrow p^+ doped region, about 0.1 μm wide, at the source side of the channel as shown in Fig. 1, improving hot-electron reliability, stabilizing the threshold voltage with scaling and reducing the punch-through voltage. [3] FIBMOS also exhibits high Early voltage, important for analog applications. Other types of MOSFETs with asymmetric channel doping profiles show good performance.[4, 5] FIB, however, provides better control of channel dopants than other approaches, *e.g.*, angle implant or diffusion from heavily doped regions.

2 OPTIMIZATION OF FIBMOS

FIBMOSs have an asymmetric channel doping profile. The channel doping for one-step FIBMOS has the step shape shown in Fig. 1. Such a profile influences the device performance. For example, the threshold voltage is a function of not only the step doping density but also the step doping width.

This function is not simple, because it is nonlinear in those two parameters. No explicit expression for the relationship exists. Hence, we have concentrated our efforts on understanding the relationship between the doping profile and the threshold voltage by simulating FIBMOSs with

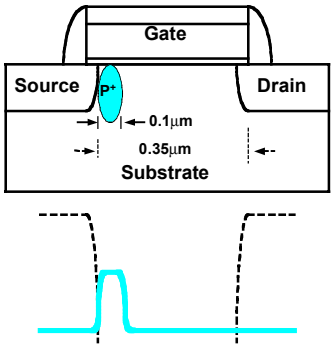

Fig. 1 Schematic for the structure and doping profile of the FIBMOS channel.

various step widths and doping densities to extract threshold voltages. The Silvaco device simulator ATLAS was used for the modeling work. For best accuracy, as many MOSFET models as possible were used. Then, the threshold voltages were mapped on a plane of step width and step doping density. In other words, three-dimensional contour plots for threshold voltage were generated with the step width on the horizontal and the step doping density on the vertical axis. Needless to say, a high-resolution contour plot is required. For each variable, more than 10 data points are needed for a decent resolution. This requires at least 100 simulations. Automation was devised to run more than 100 simulations. The automation was obtained with Perl programming. The simulation flow chart automated with Perl programming is illustrated in Fig. 2. The computer language Perl is well suited for text and this strength was fully used to write input decks for the device simulator, take the data from the simulator to write a rearranged set of data after simulation and feed graphing tools such as Kaleidagraph or MATLAB with the new set of data. Perl also has strength in system control. This strength was also used to run the device simulator as soon as the input deck was written and to arrange extracted parameters or output files in proper files or directories. The extracted threshold voltages are rearranged and fed into MATLAB for contour plots. Such a contour plot is shown in Fig. 3. From the figure, we find combinations of step doping width and doping density giving a certain threshold voltage, *e.g.*, 0.69V. The combinations of 'good parameters' are listed in Table 1. We have listed only four choices for a one-step FIBMOS that show best performance. Those four combinations of doping parameters do not result in the same performance even though the threshold voltage is the same at 0.69V. It should be noted that the current is reduced as we go from high and narrow doping profiles to low and wide doping profiles.

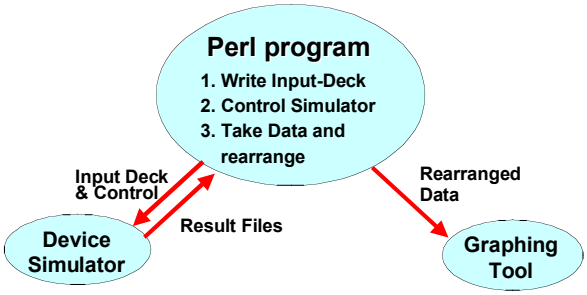

Fig. 2 Flow chart for the simulation for V_T mapping with Perl automation.

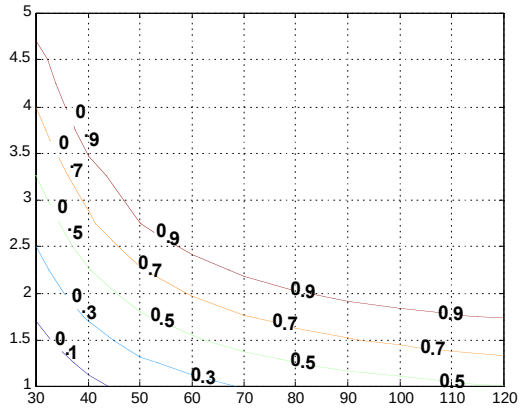

Fig. 3 Contour plots for one-step FIBMOS with channel length of 0.25µm; the numbers on the contour lines represent threshold voltages.

Two different simulations were carried out for this research. Ultimately, we need I_D–V_D and I_{sub}–V_G curves, structure files for potentials and parameters such as V_T, drain conductance, transconductance, sub-threshold swing etc. However, with all the MOSFET models used for this study, running over 100 simulations for those many outputs is very time consuming. For better efficiency, we have separated the simulations into two parts. A simple simulation, that only extracts V_T, was used for mapping and a much longer and more comprehensive simulation, was used to obtain all the outputs for only those parameter sets that were found during V_T mapping. The I_D–V_D curves from the comprehensive simulation for those four different step doping parameters in Table 1, are shown in Fig. 4 along with those of a normal MOSFET. It is clearly seen that FIBMOSs have higher drain current. It should be noted that the FIBMOS drain current is dependent on the doping profile. Fig. 5 shows substrate currents of a normal MOSFET and FIBMOSs. The substrate current is a good indicator of hot carrier degradation. It is common practice to measure substrate currents for n channel MOSFETs and gate currents for p channel MOSFETs to characterize hot carrier degradation.[6]

The substrate currents of FIBMOSs are significantly lower than those of normal MOSFETs, as shown in Fig. 5. Substrate current is also dependent on the shape of the doping steps. The substrate current increases as the doping profile changes from high and narrow to low and wide doping steps. When these doping profiles change, the threshold voltage and operation frequency (cut-off frequency) also change, but the advantages over normal MOSFET are preserved.

3 TWO-STEP FIBMOS

We observe the most beneficial effects at the step of the doping discontinuity in one-step FIBMOSs. Since FIB has the capability of defining lines as narrow as 40 nm, it allows two doping steps to be formed in the channel as shown in Fig. 6.

Step doping width (nm)	60	80	100	120
Step doping density ($\times 10^{18}$ cm^{-3})	1.95	1.61	1.43	1.32
I_D (µA/µm) at V_G = 1.8V	94.81	93.18	90.76	88.15

Table 1 Parameters for step doping giving a threshold voltage of 0.69 V. L=0.25µm.

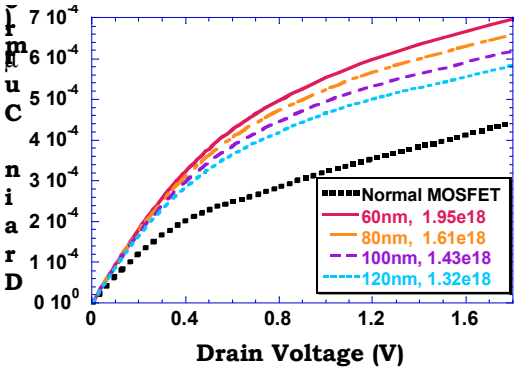

Fig. 4 I_D – V_D curves for a normal MOSFET and one-step FIBMOSs with doping parameters of Table 1. L=0.25µm and V_G = 1.8 V.

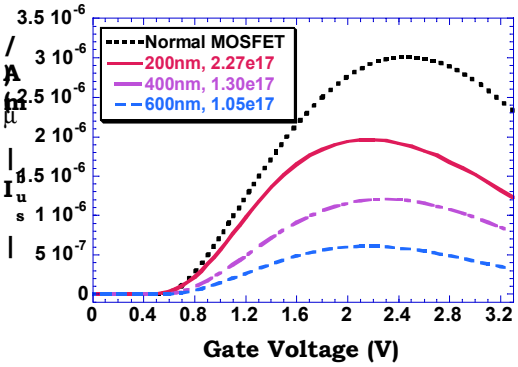

Fig. 5 I_{sub}-V_G curves for a normal MOSFET and one-step FIBMOSs. L=1.2µm.

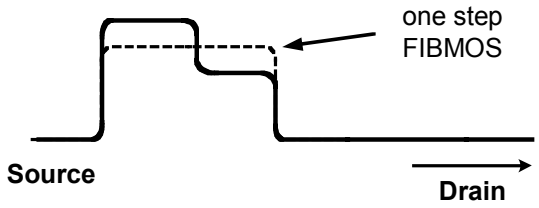

Fig. 6 Two-step FIBMOS; breaking the doping step of one-step FIBMOS into two steps leaving V_T unchanged.

First step width (nm)	30	30	40	40	40
First step doping density ($\times 10^{18}$ cm^{-3})	3.30	3.50	2.30	2.50	2.50
V_T (V)	0.609	0.595	0.589	0.590	0.590
Second step width (nm)	50	50	40	40	50
Second step doping density ($\times 10^{17}$ cm^{-3})	3.90	2.90	3.90	2.40	2.30
V_T (V)	0.687	0.691	0.688	0.690	0.688

Table 2. First step doping parameters for $V_T \approx 0.6$ V and second step doping parameters for $V_T = 0.69$ V.

The second step results in an additional electric field peak in the channel, providing another "push" for carrier drive. The additional doping step also improves V_T roll-off and drain-induced barrier lowering (DIBL). The second doping density is lower than the first with the channel doping density profile decreasing from source to drain. It is not a simple task to determine the doping density width of two-step FIBMOSs. Our approach is to find a doping profile for one-step FIBMOSs with a V_T lower than the target - we used 0.6 V - and chose another doping step for V_T to be 0.69 V. In Fig. 3, data points along the contour line of 0.6 V are chosen for the first step. The 0.6 V line is formed along the parameter combinations in Table 2, which also contains parameters of the second step to increase V_T to 0.69 V. The doping profile for the second step, however, is not unique.

We observed that many different doping profiles yield a given V_T for one step FIBMOSs and this applies to the second step, too. Although we have used as much device knowledge and scientific methodologies as possible, some degree of trial and error was inevitable to set the V_T of two step FIBMOSs at exactly 0.69 V. Perl programming, discussed earlier, makes this trial and error approach easier.

Iteration loops were set up so that nine different sets of second step parameters were tried. Nine sets are combinations of three different step widths and three different step doping densities. Even though additional iterations yield better accuracy, we cannot increase the number of iterations arbitrarily because we have to do this for several different first steps making the calculations very time consuming.

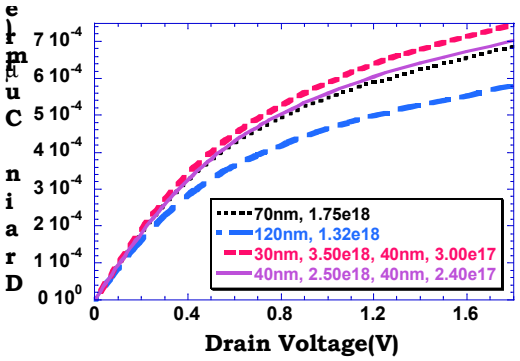

Fig. 7 I_D-V_D characteristics of representative one-step and two-step FIBMOSs. $V_G = 1.8$ V. L=0.25µm.

If a point with V_T close to 0.69 V is found by iteration, trial and error is used. The second step parameters found in this algorithm are shown in Table 2. The second step is expected to drive more current but the effective channel length is another important factor that needs to be considered. At the gate voltage that inverts the most heavily doped region, the channel on the drain side is highly inverted. Hence, the drain side of the channel behaves as an extension of the drain effectively reducing the channel length. The second step region is also highly inverted, containing more inversion carriers than the first step region but not as many as the drain side of the channel. As a result, the second step is not as effective as the drain side to reduce the effective channel length. Therefore, we can say the effective channel length is 'the first step width plus α times the second step width plus β times the unimplanted part, whereas the effective channel length for one-step FIBMOSs is 'first step width plus β times the unimplanted part', where α and β lie between 0 and 1 but α is close to unity and β is close to zero. Hence, two-step FIBMOSs have shorter effective channel lengths than one-step FIBMOSs.

We have verified that two-step FIBMOSs have higher channel electric fields and shorter effective channel lengths than one-step FIBMOSs. This explains why two-step FIBMOSs exhibit higher drain currents than one-step FIBMOSs. Fig. 7 shows the I_D-V_D characteristics of representative one-step and two-step FIBMOSs. The two representative FIBMOSs are two extreme cases. One has the highest and narrowest step doping profile and the other has the lowest and widest step doping profile that we considered. We already know that the high, narrow step doping profile gives higher drain current. Two-step FIBMOSs also have show reduced hot carrier behavior. The lateral electric field at the channel/drain junction of two-step FIBMOSs is the same as that of one-step FIBMOSs because the substrate doping density is the same for both. However, hot carriers generated at the Hi-Lo junctions between the steps, differ. In one-step FIBMOSs, the change from the step to the unimplanted region is quite large and the high electric field created at that junction generates hot carriers.

On the other hand, in two-step FIBMOSs, the electric fields at each Hi-Lo junction aids electron drift yielding

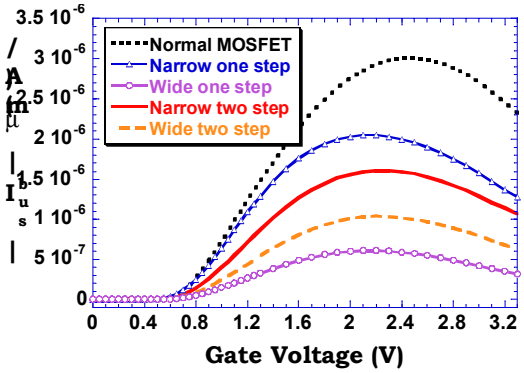

Fig. 8 Substrate current of a normal MOSFET, one-step FIBMOSs and two-step FIBMOSs for L=1.2µm.

higher currents but these are not as high as those of one-step FIBMOSs. Furthermore, before the electrons begin to be accelerated by the second electric field peak, there is a chance for relaxation at the second step with a fairly flat potential. The simulated substrate currents for a normal MOSFET, one-step FIBMOSs and two-step FIBMOSs are shown in Fig. 8.

4 LOW VOLTAGE PERFORMANCE

We have shown the superiority of FIBMOSs at a given supply voltage. Potential energy diagrams at low voltages showed that operation in the low-voltage, low-power regime is even more promising. The drain currents and the substrate currents for FIBMOSs and a normal MOSFET for different system voltages are compared in Figs. 9 and 10, respectively, by benchmarking their performance against normal MOSFETs. In this figure, I_D(FIBMOSs)/I_D(normal MOSFET) and I_{sub}(FIBMOSs)/I_{sub}(normal MOSFET) at each system voltage is used as the figure of merit. As the system voltage decreases, the FIBMOSs perform better.

5 CONCLUSIONS

We have proposed an optimizing technique for one-step FIBMOSs. Using 3-D contour plots with step doping width and doping density, we determine the doping profiles that set the threshold voltage at the targeted value for best performance. In the course of this optimization study, three new facts were discovered. First, we can choose either reliability or high drain current by changing the doping profile. If the system requirement is chiefly high current or low power, we choose narrow, high doping profiles. If the system requires long device lifetime (low hot carrier generation) and drain current can be sacrificed, wide, low-doping profiles are best. Second, breaking the doping step into two steps improves the device performance further. The optimum doping profile for two-step FIBMOSs is determined by the same techniques as those for one-step FIBMOSs. It simply requires two runs with additional trial and error. Third, FIBMOSs performance improves with reduced system voltage, *i.e.*, the drain current increases and hot carrier degradation decreases, making this technology very promising for low-power applications.

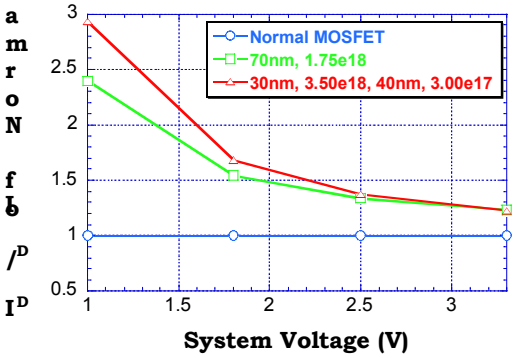

Fig. 9 Normalized drain current of FIBMOSs compared to normal MOSFET for 0.25 µm channel length.

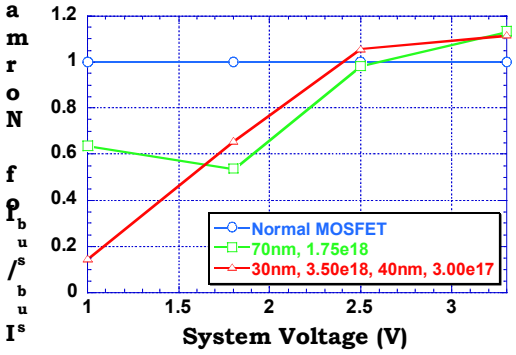

Fig. 10 Normalized substrate current of FIBMOSs compared to normal MOSFETs for 0.25 µm channel length.

REFERENCES

[1] Melngailis, J., *Focused ion beam technology and applications.* Journal of Vacuum Science & Technology B (Microelectronics Processing and Phenomena), 1987. **5**(2): p. 469-495.

[2] Kubena, R.L., J.Y. Lee, and R.A. Jullens, *Review of recent developments in focused ion beam applications.* Digest of Technical Papers - Symposium on VLSI Technology, 1984: p. 68-69.

[3] Shen, C.-C., *et al.*, *Use of focused-ion-beam and modeling to optimize submicron MOSFET characteristics.* IEEE Transactions on Electron Devices, 1998. **45**(2): p. 453-459.

[4] Ma, J., *et al.*, *Graded-channel MOSFET (GCMOSFET) for high performance, low voltage DSP applications.* IEEE Transactions on Very Large Scale Integration (VLSI) Systems, 1997. **5**(4): p. 352-9.

[5] Lyu, J., *et al.*, *Reduction of hot-carrier generation in 0.1-µm recessed channel nMOSFET with laterally graded channel doping profile.* IEEE Electron Device Lett, 1997. **18**(11): p. 535-537.

[6] Yue, J.T., *Reliability*, in *ULSI Technology*, C.Y. Chang and S.M. Sze, Editors. 1996, McGraw-Hill: New York. p. 657.

This work was supported by DoD Microelectronics Research Laboratory.